American Mineralogist, Volume 70, pages 1248–1252, 1985

Electron ordering in ilvaite, a mixed-valence iron silicate: crystal structure refinement at 138 K

SUBRATA GHOSE

Department of Geological Sciences
University of Washington, Seattle, Washington 98195

P. K. SEN GUPTA

Department of Geology
Memphis State University, Memphis, Tennessee 38152

AND E. O. SCHLEMPER

Department of Chemistry
University of Missouri, Columbia, Missouri 65211

Abstract

Ilvaite, a mixed valence iron silicate with the chemical composition, $Ca(Fe^{2+}, Fe^{3+})Fe^{2+}Si_2O_8(OH)$, shows considerable thermally activated electron delocalization among Fe^{2+} and Fe^{3+} ions located in octahedral A sites. An electron ordering induced displacive phase transition takes place from orthorhombic (space group *Pnam*) to the monoclinic (space group $P2_1/a$) symmetry upon cooling through the range 333–343 K (Ghose et al., 1984a). The crystal structure of ilvaite from Elba, Italy [$a = 13.008(1)$, $b = 8.784(1)$ $c = 5.836(1)$Å, $\beta = 90.21(1)°$] has been refined at 138 K based on 1750 reflections measured on an automatic X-ray single crystal diffractometer ($R = 0.024$). The average octahedral distances at Ao and Am sites are Ao–O = 2.101Å, Am–O = 2.048Å. Calculated effective valence charges compared to earlier room temperature results (Finger et al., 1982) indicate a slight increase of Fe^{3+} content at the Am site. Concomittant with electron ordering in A sites, the two silicate tetrahedra undergo slight, but significant changes in configuration including small changes of Si–O bond lengths.

Introduction

Ilvaite is a black mixed-valence iron silicate mineral, which shows considerable thermally activated electron delocalization between Fe^{2+} and Fe^{3+} ions in octahedral sites, reminiscent of the situation in magnetite. The chemical composition of ilvaite can be represented as:

$$\langle Ca\rangle\{Fe^{2+},Fe^{3+};Fe^{2+}\}[Si_2]O_8(OH).$$

where ⟨ ⟩, { }, and [ ], brackets indicates cations in seven-fold, octahedral and tetrahedral coordination, respectively. The crystal structure consists of edge-sharing double chains of octahedra (the A sites) running parallel to the **c** axis. Half as many larger octahedra (B sites) are attached along the chains, sharing edges with A site octahedra. Ca^{2+} ions and Si_2O_7 groups interconnect these chains (Fig. 1). Ferric and ferrous ions occur in equivalent A sites in the orthorhombic phase, which facilitates electron hopping between them.

Electron delocalization and phase transitions in ilvaite

A considerable amount of Mössbauer spectroscopic study has been carried out in the temperature range where electron fluctuations ($Fe^{2+} \leftrightarrow Fe^{3+}$) are important, from which the electron ordering seems to take place at around 400 K (e.g., see Heilman et al., 1977; Evans and Amthauer, 1980) and the activation energy of the electron hopping has been estimated to be 0.11 eV from a relaxation model (Litterst and Amthauer, 1984) and 0.13 eV from electrical conductivity measurements (‖c) in single crystals (Coey et al., 1984).

Recent X-ray and neutron diffraction studies indicate that at room temperature ilvaite is monoclinic (space group $P2_1/a$), where a mirror plane in the high temperature orthorhombic structure (space group *Pnam*) is lost, and the A sites split up into inequivalent sites, each of which principally accomodates Fe^{2+} or Fe^{3+} ions (Finger et al., 1982; Takéuchi et al., 1983; Ghose et al., 1984b). From high temperature X-ray powder diffraction studies with a Guinier camera, the orthorhombic to monoclinic phase transition has been located in the range 333–343 K (Ghose et al., 1984a). The very small deviation of the monoclinic structure ($\beta = 90.25°$) from orthorhombic symmetry explains why a number of earlier X-ray and neutron structure determinations on single crystals at room temperature were made assuming the orthorhombic symmetry (Belov and

0003–004X/85/1112–1248$02.00

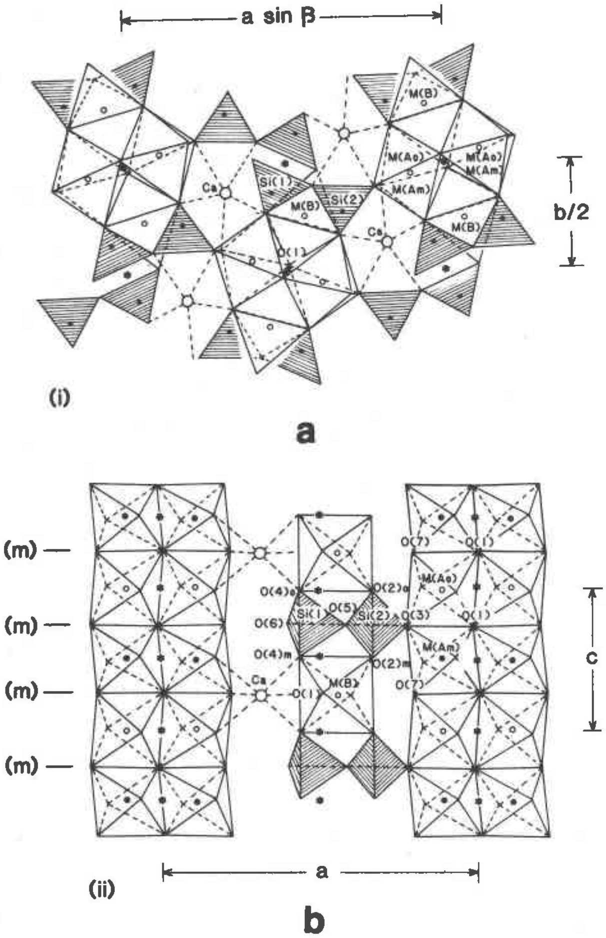

Fig. 1. The crystal structure of ilvaite (a) projection down the **c** axis, (b) partial view of the structure down the *b* axis. M(Ao) and M(Am) sites are shown as open and filled circles respectively; *m* indicates pseudo-mirror plane (modified after Takéuchi, Haga and Bunno, 1983).

Mokeeva, 1954; Beran and Bittner, 1974; Haga and Takéuchi, 1976), although careful X-ray powder diffraction studies indicated monoclinic symmetry (Bartholomé et al., 1968; Dietrich, 1972) For a while, it was believed that ilvaite exists in *both* orthorhombic and monoclinic forms at room temperature. It is now clear that the orthorhombic to monoclinic phase transition is thermally induced by electron ordering, a phenomenon closely comparable to the Verwey transition at 118 K in magnetite (Verwey and Haymaan, 1941) from cubic to the monoclinic symmetry, accompanied by a considerable loss in electrical conductivity.

In addition, ilvaite shows two magnetic phase transitions at 116 K (Yamanaka and Takéuchi, 1979; Coey et al., 1984) and 40 K (Coey et al., 1984; Ghose et al., 1984a) determined from magnetic, specific heat and Mössbauer measurements. Magnetic structures below these two phase transitions (at 80 K and 5 K) have been determined from powder neutron diffraction (Ghose, Hewat and Marezio, 1984). At 80 K, the spins on the Fe^{2+} and Fe^{3+} ions in A sites are ordered, whereas those on Fe^{2+} ions in B sites are essentially disordered; at 5 K, spins on Fe^{2+} ions on B sites are ordered as well.

The powder neutron diffraction study of ilvaite from 305 to 5 K indicated a progressive increase in electron ordering with decreasing temperature in the monoclinic phase (Ghose et al., 1984b). Because the precision of structure determination by the Rietveld profile fitting of the powder neutron diffraction data is not very high, the present low temperature single crystal X-ray diffraction study was undertaken to check further the earlier neutron results. Room temperature refinements of the monoclinic ilvaite structures have been carried out by Finger et al. (1982) and Takéuchi et al. (1983), with which our results can be compared.

Experimental

For the X-ray diffraction experiment at 138 K, an ilvaite specimen from Elba, Italy (Dartmouth College, #DP 631-7) was used, the same one used by Finger et al. (1982), who determined the chemical composition to be $CaFe_{2.73}Al_{0.12}Mn_{0.07}Mg_{0.04}Si_2O_8(OH)$. A prismatic crystal, $0.10 \times 0.13 \times 0.13$ mm, was mounted on the Enraf-Nonius CAD-4 diffractometer equipped with a low temperature cooling device using a stream of cold nitrogen gas. The temperature stability is ± 1 K. The unit cell dimensions (Table 1) were determined from 2θ values of reflections with $20° < 2\theta < 40°$(Mo$K\alpha$ 0.70926Å). A total of 3496 reflections with $2\theta < 60°$ were collected, which yielded 1939 unique reflections [1750 with $F_0 > 2\sigma(F_0)$]. Absorption corrections were made by the empirical (psi-scan) method.

Full matrix least squares refinement of the structure was carried out on a PDP 11/34 computer using the Enraf-Nonius SDP programs. The positional and isotropic thermal parameters given by Finger et al. (1982) served as input parameters. Atomic scattering factors for Ca, Fe, Si and including f′ and f″ values were taken from *Tables for X-ray Crystallography* (v. IV, 1974) and for H from Stewart, Davidson and Simpson (1965). The hydrogen position was directly determined from difference Fourier maps. Anisotropic temperature factors for all atoms were used except for hydrogen. The final *R*-factor is 0.024 (weighted $R = 0.035$) for 1750 reflections. The atomic positional and equivalent isotropic thermal parameters are listed in Table 2, the bond lengths and angles with standard deviations in Table 3, and anisotropic temperature factors and the F_0–F_c list in Table 4.[1]

Results and discussion

Electron ordering and the monoclinic beta angle

Takéuchi et al. (1983) have correlated the degree of electron order σ with the β angle in ilvaite based on structure refinements of two different samples (Techukhe, Siberia and Tsumo, Japan) at room temperature and concluded that the ideal β angle for completely ordered ilvaite should be 90.45°. This result is in contradiction with the powder neu-

---

[1] To receive a copy of Table 4, order Document AM-85-289 from the Business Office, Mineralogical Society of America, 2000 Florida Avenue, N.W., Washington, D.C. 20009. Please remit $5.00 in advance for the microfiche.

Table 1. Ilvaite: crystal data

Ilvaite, $CaFe_{2.72}Al_{0.12}Mn_{0.07}Mg_{0.04}Si_2O_8(OH)$

Elba, Italy (Dartmouth College DP 631-7)

	138K	298K (Finger et al. 1982)
a(Å):	13.008 (1)	13.0103 (5)
b(Å):	8.784 (1)	8.8039 (4)
c(Å):	5.836 (1)	5.8517 (3)
β(°):	90.21 (1)	90.209 (5)
V(Å^3):	666.83	670.26
Space group:	$P2_1/a$	$P2_1/a$
μ_{MoK_α} (cm^{-1})	76.6	76.6
No. of refl.:	1750	1735
R:	0.024	0.032
R_w:	0.035	0.040

tron diffraction refinements of ilvaite from Seriphos, Greece, where at 5 K the electron ordering is very nearly complete and the β angle is 90.23°, the latter varying very little with temperature (Ghose et al., 1984b). In the present study on the Elba sample, the β angle is identical at 298 and 138 K. Hence, differences in β angles cannot be used as reliable indicators of electron order as proposed by Takéuchi et al. (1983). Rather, the explanation for the variation in β angles observed in various ilvaite single crystals most probably lies in the fine scale twinning, associated with the displacive orthorhombic to monoclinic phase transformation which all natural ilvaites must have undergone.

Table 2. Positional parameters and their estimated standard deviations

ATOM	x	y	z	B(Å^2)
Fe(1)(Ao)	0.89001(2)	0.05004(4)	0.00852(5)	0.320(5)
Fe(2)(Am)	0.88996(2)	0.05218(4)	0.49051(5)	0.307(5)
Fe(3)(B)	0.94134(2)	0.74089(4)	0.24923(6)	0.307(5)
Ca	0.81261(3)	0.37020(5)	0.75256(8)	0.316(7)
Si(1)	0.95954(5)	0.36916(7)	0.2492(1)	0.233(9)
Si(2)	0.67914(5)	0.22764(7)	0.2518(1)	0.231(9)
O(1)	0.0090(1)	0.0294(2)	0.7379(3)	0.51(3)
O(2)o	0.9369(1)	0.2722(2)	0.0159(3)	0.35(3)
O(2)m	0.9354(1)	0.2728(2)	0.4829(3)	0.34(2)
O(3)	0.7774(1)	0.1102(2)	0.2553(3)	0.33(3)
O(4)o	0.6706(1)	0.3289(2)	0.0179(3)	0.37(3)
O(4)m	0.6703(1)	0.3318(2)	0.4830(3)	0.36(3)
O(5)	0.5848(1)	0.1008(2)	0.2524(3)	0.33(3)
O(6)	0.6018(1)	0.0264(2)	0.7519(3)	0.43(3)
O(7)	0.7980(1)	0.1096(2)	0.7441(3)	0.36(2)
H	0.741(3)	0.098(6)	0.743(7)	3.2(9)

Starred atoms were refined isotropically.
Anisotropically refined atoms are given in the form of the Isotropic equivalent thermal parameter defined as:

$$4/3\ \beta_{11}a^2 + \beta_{22}b^2 + \beta_{33}c^2 + \beta_{12}\,ab\cos\gamma + \beta_{13}\,ac\cos\beta + \beta_{23}\,bc\cos\alpha$$

Site nomenclature

The orthorhombic to monoclinic phase transition in ilvaite is displacive, the monoclinic space group $P2_1/a$ being a subgroup of the orthorhombic space group *Pnam*. Below T_c, the mirror plane normal to **c** in the orthorhombic phase is lost, but continues to serve as a pseudo-mirror plane in the monoclinic structure and the octahedral A site splits up into two inequivalent sites, which we will call Ao and Am [or M(Ao) and M(Am); cf. feldspars, Megaw, 1956]; O(2) and O(4) atoms likewise split up into O(2)o, O(2)m and O(4)o and O(4)m. This nomenclature has the advantage of indicating the genetic structural relationships of the atoms concerned above and below the phase transition.

Electron ordering in the octahedral sites as a function temperature

The bond lengths and angles at 138 K are shown along with those determined at room temperature by Finger et al. (1982) in Table 3. The precisions of both determinations are closely comparable. Ghose et al. (1984b) have calculated the effective valence charges **S** (Zachariasen, 1978) according to the empirical formula of Brown and Shannon (1973) and Brown and Wu (1976).

$$\mathbf{S} = \sum_i \mathbf{s}_i = \sum_i \left(\frac{R_{\mathrm{Me-Oi}}}{R_{\mathrm{Me-O}}}\right)^{-N_{\mathrm{Me}}}$$

where R_{Me-O} and N_{Me} are empirical constants tabulated for various metal cations Me, where the summation is over all bond lengths, R_{Me-O_i}. For Fe^{2+} and Fe^{3+} ions in octahedral coordination these values are: $R_{Fe^{3+}-O} = 1.764$, $N_{Fe^{2+}} = 5.5$ and $R_{Fe^{3+}-O} = 1.780$, $N_{Fe^{3+}} = 5.7$. The **S** values calculated for both data sets at *RT* and 138 K indicate a small, but significant increase in the Fe^{3+} ion content at the Am site at 138 K in conformity with the trend reported by Ghose et al. (1984b). Although a major portion of the itinerant electrons are ordered during the orthorhombic to monoclinic phase transition, the rest of the electrons seem to order slowly with decreasing temperature; ordering is completed at a temperature very close to 0 K. As expected, the **S** values for the Fe^{2+} ions (with a small amount of Mn^{2+}) at the B site change very little with temperature.

Electron ordering and configuration of the silicate tetrahedra

As indicated earlier, the diorthosilicate $[Si_2O_7]$ groups interconnect the double octahedral chains. The electron ordering in the Ao and Am sites by principally Fe^{2+} and Fe^{3+} ions manifests itself through the splitting of Si(1)–O(2) and Si(2)–O(4) bonds into two sets: Si(1)–O(2)o and Si(1)–O(2)m, and Si(2)–O(4)o and Si(2)–O(4)m in the monoclinic phase; in addition to Ca and Fe in the B site, O(2)o [and likewise, O(4)o] is bonded to Fe^{2+} at Ao, whereas O(2)m is bonded to Fe^{3+} at Am. The ensuing valence charge difference requires that the Si(1)–O(2)o distance be shorter than the Si(1)–O(2)m distance [likewise, Si(2)–O(4)o and Si(2)–O(4)m], which is the case both at *RT* and 138 K

Table 3. Ilvaite; interatomic distances (Å) and angles (°) (with standard deviations in parentheses)

Bond lengths		138K	298K[1]
M(Ao)	- O(1)	2.093(2)	2.086(2)
	- O(1)	2.219(2)	2.222(2)
	- O(2)(O)	2.046(2)	2.053
	- O(3)	2.122(2)	2.126(2)
	- O(4)(O)	2.103(2)	2.114(2)
	- O(7)OH	2.020(2)	2.017(2)
	mean	2.101	2.103
	S	2.332	2.319
M(Am)	- O(1)	2.006(2)	2.017(2)
	- O(1')	2.119(5)	2.132(2)
	- O(2)(m)	2.027(2)	2.036(2)
	- O(3)	2.064(2)	2.080(2)
	- O(4)(m)	2.096(2)	2.102(2)
	- O(7)OH	1.974(5)	1.976(2)
	mean	2.048	2.057
	S	2.732	2.662
M(B)	- O(1)	2.122(2)	2.128(2)
	- O(2)(O)	2.219(2)	2.229(2)
	- O(2)(m)	2.237(2)	2.246(2)
	- O(4)(O)	2.263(2)	2.270(2)
	- O(4)(m)	2.280(2)	2.287(2)
	- O(6)	1.967(2)	1.966(2)
	mean	2.181	2.188
	S	1.963	1.938
Ca	- O(2)(O)	2.384(2)	2.392(2)
	- O(2)(m)	2.402(4)	2.408(2)
	- O(3)	2.414(2)	2.413(2)
	- O(4)(O)	2.438(2)	2.449(2)
	- O(4)(m)	2.445(2)	2.457(2)
	- O(5)	2.427(2)	2.424(2)
	- O(7)OH	2.301(2)	2.303(2)
	mean	2.402	2.407
Si(1)	- O(2)(O)	1.630(2)	1.630(2)
	- O(2)(m)	1.635(2)	1.636(2)
	- O(5)	1.651(2)	1.657(2)
	- O(6)	1.595(2)	1.599(2)
	mean	1.628	1.630
Si(2)	- O(3)	1.643(2)	1.644(2)
	- O(4)(O)	1.631(2)	1.629(2)
	- O(4)(m)	1.633(2)	1.632(2)
	- O(5)	1.653(2)	1.656(2)
		1.640	1.640
H...	O(6)	1.923	1.98
H...	O(7)	0.743	0.84

Bond angles[2]		138K	298K[1]
M(Ao):	O(1)-O(1)	92.18(6)	92.05(9)
	O(1)-O(2)(O)	83.38(6)	83.45(9)
	O(1)-O(3)	170.24(7)	170.33(9)
	O(1)-O(4)(O)	97.71(6)	97.87(9)
	O(1)-O(7)	83.71(6)	84.29(9)
	O(1')-O(2)(O)	96.71(7)	96.81(9)
	O(1')-O(3)	92.08(6)	91.84(9)
	O(1')-O(4)(O)	88.74(6)	88.58(9)
	O(1')-O(7)	174.26(7)	174.46(9)
	O(2)(O)-O(3)	87.40(7)	87.30(9)
	O(2)(O)-O(4)(O)	174.40(7)	174.41(9)
	O(2)(O)-O(7)	86.82(7)	86.91(9)
	O(3)-O(4)(O)	91.16(6)	91.07(9)
	O(3)-O(7)	92.60(6)	92.42(9)
	O(4)(O)-O(4)(O)	87.84(6)	87.81(9)
M(Am):	O(1)-O(1')	86.58(5)	87.24(9)
	O(1)-O(2)(m)	97.76(5)	97.54(9)
	O(1)-O(3)	96.36(7)	95.25(9)
	O(1)-O(4)(m)	88.01(7)	87.86(9)
	O(1)-O(7)	171.91(5)	172.61(9)
	O(1')-(2)(m)	83.87(5)	83.91(5)
	O(1')-O(3)	171.15(5)	171.03(5)
	O(1')-O(4)(m)	97.74(5)	97.97(9)
	O(1')-O(7)	87.52(5)	87.67(9)
	O(2)(m)-O(3)	87.46(7)	87.22(9)
	O(2)(m)-O(4)(m)	174.11(7)	174.38(9)
	O(2)(m)-O(7)	87.11(5)	87.25(9)
	O(3)-O(4)(m)	90.71(6)	90.74(9)
	O(3)-O(7)	90.29(5)	90.60(9)
	O(4)(m)-O(7)	87.30(5)	87.54(9)

Table 3. (cont.)

Bond angles		138K	298K
M(B):	O(1)-O(2)(O)	81.72(6)	81.61(9)
	O(1)-O(2)(m)	78.99(6)	79.15(9)
	O(1)-O(4)(O)	83.94(6)	83.60(9)
	O(1)-O(4)(m)	80.63(6)	80.60(9)
	O(1)-O(6)	177.82(7)	177.99(9)
	O(2)(O)-O(2)(m)	88.44(6)	88.55(9)
	O(2)(O)-O(4)(O)	89.79(6)	89.59(9)
	O(2)(O)-O(4)(m)	162.27(6)	162.17(9)
	O(2)(O)-O(6)	98.75(7)	98.84(9)
	O(2)(m)-O(4)(O)	162.92(7)	167.73(9)
	O(2)(m)-O(4)(m)	89.80(6)	89.36(9)
	O(2)(m)-O(6)	98.88(6)	98.90(9)
	O(4)(O)-O(4)(m)	86.73(6)	87.17(9)
	O(4)(O)-O(6)	98.18(7)	98.35(9)
	O(4)(m)-O(6)	94.95	94.44(9)
Si(1):	O(2)(O)-O(2)(m)	113.00(9)	113.28(12)
	O(2)(O)-O(5)	105.57(9)	105.62(12)
	O(2)(O)-O(6)	111.10(9)	110.97(12)
	O(2)(m)-O(5)	105.40(9)	105.35(12)
	O(2)(m)-O(6)	110.71(9)	110.66(12)
	O(5)-O(6)	110.80(8)	110.70(12)
Si(2):	O(3)-O(4)(O)	113.79(9)	113.69(12)
	O(3)-O(4)(m)	113.49(9)	113.73(12)
	O(3)-O(5)	98.85(9)	98.64(12)
	O(4)(O)-O(4)(m)	112.35(8)	112.40(12)
	O(4)(O)-O(5)	108.65(9)	108.79(12)
	O(4)(m)-O(5)	108.65(8)	108.49(12)
	O(7)-O(6)	168.73	

[1] Data from Finger, Hazen, and Hughes (1982).

[2] Bond angles around M(Ao), etc.: for O(1)-O[1] read O(1) - M(Ao) - O(1).

for our specimen from Elba (Table 3), as well as, for the ilvaite specimen from Tsumo, Japan (Takéuchi et al., 1983). Hence, this effect, albeit small, is significant. This is the first known instance, where electron ordering in adjacent Fe sites induces configurational changes in silicate tetrahedra.

Both silicate tetrahedara are distorted from a regular shape. Although the two bridging Si(1)–O(5) (1.650Å) and Si(2)–O(5) (1.658Å) bonds are nearly equal, the two terminal bonds, Si(1)–O(6) = 1.595Å and Si(2)–O(3) = 1.643Å are greatly different from each other due to the fact that O(6), in trigonal planar coordination with Si(2), Fe^{2+} at the B site and H, is grossly underbonded, whereas O(3) in tetrahedral coordination is nearly charge balanced. Furthermore, sharing of the tetrahedral edge O(3)–O(5) with the Ca^{2+} polyhedron causes the O(3)–Si(2)–O(5) angle = 98.9° to be unusually small, which contributes substantially to the lengthening of the Si(2)–O(3) bond compared to the expected value of a terminal bond, 1.62–1.63Å. Apart from the slight differences due to electron ordering mentioned earlier, pairs of Si(1)–O(2) and Si(2)–O(4) bonds are nearly equal, reflecting very similar tetrahedral coordination of O(2) and O(4) atoms.

Hydrogen bond

Within the OH group, O(7) is tetrahedrally coordinated, the O–H distance being 0.75Å, which is somewhat shorter than expected. O(6), in trigonal planar coordination, is the recipient of the hydrogen bond, the H ··· O(6) distance being 1.92Å. In spite of the large uncertainties in the determination of the hydrogen position, the O–H distance determined by X-ray diffraction is significantly shorter than the value 0.985Å determined by neutron diffraction (in the supposedly orthorhombic phase) by Haga and Takéuchi (1976). This difference indicates that the electron cloud of the hydrogen atom is much closer to the bonded oxygen, O(7) than the proton.

Acknowledgments

We are indebted to Dartmouth College for the donation of the ilvaite specimen. This research has been supported in part by the NSF grant EAR 82-06526 (S. Ghose).

References

Bartholomé, P., Duchesne, J. C. and Van der Plas, L. (1968) Sur une forme monoclinique de l'ilvaite. Annales de la Société Geologique de Belgique, 90, 779–788.

Belov, N. V. and Mokeeva, V. I. (1954) The crystal structure of ilvaite (in Russian). Trudy. Inst. Krist Akadamiia Nauk. SSSR, 9, 89–102.

Beran, A. and Bittner, H. (1974) Untersuchungen zur Kristallchemie des Ilvaits. Tschermaks mineralogische und petrologische Mitteilungen, 21, 11–29.

Brown, I. D. and Kun, W. K. (1974) Empirical parameters for calculating cation–oxygen bond valences. Acta Crystallographica, B32, 1957–1959.

Brown, I. D. and Shannon, R. D. (1973) Empirical bond-length bond-strength curves for oxides. Acta Crystallographica, A29, 266–282.

Coey, J. M. D., Allan, J. Xuemin, K., Van Dang, N. and Ghose, S. (1984) Magnetic and electrical properties of ilvaite. Journal of Applied Physics, 55, 1963–1965.

Dietrich, V. (1972) Ilvaite, Ferroantigorit und Greenlith als Begleiter oxidisch sulfidischer Vererzungen in den Oberhalbsteiner Serpentiniten. Schweizerische mineralogische und petrologische Mitteilungen, 52, 57–74.

Evans, B. J. and Amthauer, G. (1980) The electronic structure of ilvaite and the pressure and temperature dependence of its Fe^{57} Mössbauer spectrum. Journal of Physics and Chemistry of Solids, 41, 985–1001.

Finger, L. W., Hazen, R. M. and Hughes, J. M. (1982) Crystal structure of monoclinic ilvaite. Carnegie Institution of Washington Yearbook 81, 386–388.

Ghose, S., Hewat, A. W., Marezio, M., Dang, N. V., Robie, R. A. and Evans, H. T. (1984a) Electron and spin ordering and associated phase transitions in ilvaite, a mixed valence iron silicate. (abstr.) Transactions of the American Geophysical Union, 65, 289.

Ghose, S., Hewat, A. W. and Marezio, M. (1984b) A neutron powder diffraction study of the crystal and magnetic structures of ilvaite from 305 to 5K—a mixed valence iron silicate with an electronic transition. Physics and Chemistry of Minerals, 11, 67–74.

Haga, N. and Takéuchi, T. (1976) Neutron diffraction study of ilvaite. Zeitschrift für Kristallographie, 144, 161–174.

Heilmann, I. S., Olsen, N. B. and Olsen, J. S. (1977) Electron hopping and temperature dependent oxidation states of iron in ilvaite by Mössbauer effect. Physica Scripta, 15, 285–288.

Megaw, H. D. (1956) Notation for feldspar structures. Acta Crystallographica, 9, 56–60.

Stewart, R. F., Davidson, E. R. and Simpson, W. T. (1965) Coherent x-ray scattering for the hydrogen atom in the hydrogen molecule. Journal of Chemical Physics, 42, 3175–3187.

Takéuchi, Y., Haga, N. and Bunno, M. (1983) X-ray study of polymorphism of ilvaite $HCaFe_2^{2+}Fe^{3+}O_2$ $[Si_2O_7]$. Zeitschrift für Kristallographie, 163, 267–283.

Verwey, E. J. and Haymaan, P. W. (1941) Electronic conductivity and transition point of magnetite, (Fe_3O_4). Physica, 8, 979–987.

Yamanaka, Y. and Takéuchi, Y. (1979) Mössbauer spectra and magnetic features of ilvaites. Physics and Chemistry of Minerals, 4, 149–159.

Manuscript received, February 22, 1985;
accepted for publication, July 26, 1985.